Talanta 88 (2012) 345–351

Contents lists available at SciVerse ScienceDirect

Talanta

journal homepage: www.elsevier.com/locate/talanta

A dynamic study on reversal of multidrug resistance by ginsenoside Rh_2 in adriamycin-resistant human breast cancer MCF-7 cells

Bei Zhou, Xiuli Xiao, Lili Xu, Lian Zhu, Liang Tan*, Hao Tang, Youyu Zhang, Qingji Xie, Shouzhuo Yao

Key Laboratory of Chemical Biology and Traditional Chinese Medicine Research (Ministry of Education of China), College of Chemistry and Chemical Engineering, Hunan Normal University, Changsha, 410081, PR China

ARTICLE INFO

Article history:
Received 27 July 2011
Received in revised form 26 October 2011
Accepted 28 October 2011
Available online 2 November 2011

Keywords:
MCF-7/ADR cells
Multidrug resistance
Ginsenoside Rh_2
Cytotoxicity
Dynamic measurement

ABSTRACT

The quartz crystal microbalance (QCM) dynamic measurements indicate that ginsenoside Rh_2 (G-Rh_2) could inhibit the proliferation of adriamycin-resistant human breast cancer MCF-7 cells (MCF-7/ADR) in a concentration-dependent way. The combined treatment of G-Rh_2 with adriamycin (ADR) at non-effect dosage resulted in the higher inhibition efficiencies and the increased cell-death velocity, suggesting excellent ability of G-Rh_2 for reversal of multidrug resistance in MCF-7/ADR cells. The cytotoxic effect of the ADR–G-Rh_2 combination was evaluated with the modified Bürgi formula (Jin equation) based on the QCM responses. It presented apparent synergism, indicating the potential ability of G-Rh_2 in tumor therapy. Fluorescent microscopic inspection and methyl thiazolyl tetrazolium (MTT) assay were also carried out and exhibited the comparable results to QCM analysis. The present work may lay an experimental foundation for the application of ginsenosides in cancer therapy, especial in multidrug resistance research.

1. Introduction

Multidrug resistance (MDR) means that tumor cells growing in the presence of a single anti-cancer drug may become resistant to a wide range of structural dissimilar drugs. This resistance to therapy is correlated to the presence of some molecular "pumps" in tumor-cell membranes that actively expel chemotherapy drugs from the interior [1]. The resistance development of tumor cells to chemotherapeutic drugs is a major obstacle in the treatment of human cancer [2]. It affects patients with a variety of blood cancers and solid tumors, including breast, ovarian, lung and gastrointestinal tract cancers. Design and development of drugs that can reverse multidrug resistance in tumor cells have been one of important targets in cancer researches. Doctors usually chose drug combination in actual therapies in order to intensify therapeutic effect, avoid MDR phenomenon and reduce drug toxicity. Many reports on synergistic effect induced by drug combination have been presented [3–5].

Ginseng has been employed as a costly invigorant for thousands of years in Asian countries including China, Korea and Japan. Ginsenosides are the major effective components of ginseng and contain a similar basic structure, composed of gonane steroid nucleus having 17 carbon atoms arranged in four rings. They can be divided into two main types, the 20(S)-protopanaxatriol and 20(S)-protopanaxadiol family, according to the existence of the hydroxyl group at C-6 or not. Ginsenosides have displayed a wide variety of biological activities including immunomodulatory effects, anti-inflammatory and anti-tumor activity [6–8]. Ginsenoside Rh_2 (G-Rh_2) is isolated from red ginseng [9] and belongs to protopanaxadiol type. It exhibits notably low toxicity and few side-effects over chemotherapeutic agents [10]. Some investigations have reported that G-Rh_2 not only inhibits cell-growth via induction of the cell differentiation, but also induces Gl phasearrest and/or S phase-prolongation in tumor cell cultures [11,12]. It can inhibit growth of human colorectal cancer HCT116 and SW480 cells [13], human breast cancer MCF-7 and MDA-MB-231 cells [14] as well as hepatoma SK-HEP-1 cells [15]. Furthermore, it can also induce apoptosis in such cell lines as rat C6 glioma cells [16], human neuroblastoma SK-N-BE(2)-C cells [17] and human malignant melanoma A375-S2 cells [18]. Researchers are pleasantly surprised to find that G-Rh_2 has remarkable synergy effects to some chemotherapeutic agents, even at a non-effect dosage [19,20]. The reason for this phenomenon is usually ascribed to the potential interaction between G-Rh_2 and efflux transporters such as P-glycoprotein [21] and breast cancer resistance protein [22]. These membrane transporter proteins are one of key factors leading to MDR of tumor cells. So it is expected that G-Rh_2 has influence on multidrug resistance in tumor cells.

Conventional optical methods including microscopy observation, methyl thiazolyl tetrazolium (MTT) colorimetry and flow cytomertry (FCM) in the cell investigation have some drawbacks, e.g., multistep operation and inapplicability for real-time or

* Corresponding author. Tel.: +86 731 8887 2046; fax: +86 731 8887 2046.
E-mail address: liangtan@hunnu.edu.cn (L. Tan).

0039-9140/$ – see front matter © 2011 Elsevier B.V. All rights reserved.
doi:10.1016/j.talanta.2011.10.051

continuous monitoring besides their virtues including good reliability and accuracy. The quartz crystal microbalance (QCM) not only can provide information about mass loading but also can reveal the physico-chemical properties including density and viscosity near the electrode. As a powerful tool to monitor adsorption processes or reactions at solid/liquid interfaces in chemical and biological research, the QCM has been widely used for analyses of proteins, enzymes, antibody/antigen, nucleic acids and bacteria [23,24]. Generally, adherent cells are of tenfold μm-scale size in diameter, being much thicker than the characteristic extinction depth of the QCM shear wave ($\delta \approx 0.188$ μm for 9 MHz crystal in water [25]). The influences of resonant frequency on cell growth can be basically ignored. Due to its satisfactory performance, e.g., non-destruction measurement, high sensitivity, facile operation and dynamic monitoring, QCM has been successfully employed to monitor living cell attachment and incubation [26–29]. In our previous work, the antitumor effects of drugs and the synergistic cytotoxicity of the drug combination on hepatic cancer cells Bel7402 by QCM measurement were investigated, respectively [30]. It has proved that QCM is one of the most powerful tools available for drug toxicology research.

It can be imagined that the combination of chemotherapy drug with ginsenoside Rh_2 should exhibit different cytotoxicity to individual component and affect multidrug resistance in multidrug resistant tumor cells. To the best of our knowledge, to date there are no reports on application of QCM for dynamic study on the effect of G-Rh_2 on growth of multidrug resistant tumor cells. In this study, the antitumor effects of adriamycin, G-Rh_2 and their combination on adriamycin-resistant human breast cancer cells MCF-7 were investigated with the QCM measurement, fluorescent microscopic inspection and MTT assay, respectively. The cytotoxicity of the drug combination were also evaluated

2. Materials and methods

2.1. Chemicals and instruments

Adriamycin-resistant human breast cancer MCF-7 cells (MCF-7/ADR) were obtained from XiangYa Central Laboratory of Central South University, China and was routinely cultured using RPMI-1640 growth medium (from Gibco) supplementing with 10% newborn calf serum and 1 μmol L^{-1} ADR. 3-(4,5-dimethylthiazol-2-yl)-2,5-diphenyltetrazolium bromide (MTT) were obtained from Amresco. A pH 7.4 phosphate buffer solution consisting of 136.7 mmol L^{-1} NaCl, 2.7 mmol L^{-1} KCl, 9.7 mmol L^{-1} Na_2HPO_4, and 1.5 mmol L^{-1} KH_2PO_4 was used in cell culture. Doxorubicin hydrochloride (adriamycin, ADR) was purchased from Zhejiang Hisun Pharmaceutical Co., Ltd. (China). 20(S)-Ginsenoside Rh_2 was obtained from National Institutes for Food and Drug Control (China), and was of biochemical reagent grade and at least 95% pure as determined by HPLC. It was dissolved in ethanol and further diluted with growth medium. Its stock solution (320 μmol L^{-1}) was stored at −20 °C. Other chemicals were of analytical reagent grade.

The QCM sensor consisted of a thin AT-cut quartz crystal wafer with one gold electrode (6-mm diameter) on each side. The 9-MHz crystal with Au electrodes was mounted between two biocompatible silicon O-rings to allow only one side of the electrode to be exposed to the liquid. The reaction chamber above the crystal was held with a 1 mL chlorinated polyethylene centrifugal tube. The device, being covered, was placed in a humidified CO_2 incubator controlled at 5% CO_2 and 37 °C to prevent evaporation from the culture holder. The quartz crystal electrodes were wire-extended to a research QCM (Maxtek Inc., USA) to achieve simultaneous recording of resonant frequency (f_0) and motional resistance (R_1). The cell-modality observation was performed with an inverted optical microscope (OLYMPUS CKX41, Japan). The pictures of stained cells were observed on an inverted fluorescence microscope (NIKON Eclipse Ti-S, Japan).

2.2. Cell culture and measurement procedures

After being sterilized with 75% ethanol under UV light for 0.5 h, the QCM culture-chamber was washed thrice with PBS. Then 800 μL of the growth medium was added and the entire culture-chamber was put into the incubator. As soon as the QCM readout became steady, 200 μL of the culture medium containing a controlled number of fleshly trypsinized cells was added evenly. In order to diminish changes in liquid density and viscosity caused by difference in temperature, the cell-suspending medium was also adjusted to 37 °C before its introduction. The Δf_0 and ΔR_1 responses were simultaneously monitored up to two days. The drug was introduced at 24 h when the cells were in their growth phases. The crystal regeneration was achieved by dealing with trypsin for 24 h, followed by washing with chromic–sulphuric acid and water in sequence for several times. After cleaning in this way, the QCM electrode could be used repeatedly with good recovery of its initial f_0 and R_1 values.

2.3. MTT assay

The metabolic activity of MCF-7/ADR was determined in triplicate using the MTT cell viability assay. Cells were seeded at a density of 5×10^4 cells $well^{-1}$ and incubated with drugs. After 24 h, cells were washed with PBS and then 0.2 mL growth medium and 50 μL MTT reagents (2 mg mL^{-1}) were added into each well. The cells were allowed to grow for another 4 h until a purple precipitate was visible. The medium was then removed and 150 μL dimethyl sulphoxide was added. The well was vibrated for 10 min to completely liberate the crystals. Finally, the absorbance was measured at 570 nm.

3. Results and discussion

3.1. The modality characterization of MCF-7/ADR cells

Fig. 1 shows the microscopic photos of MCF-7/ADR cells and MCF-7 cells in logarithmic growth phase. MCF-7/ADR cells adhered on the substrate were closely interconnected, presenting vague cellular outline. They owned the increased contact area and reduced height profile than normal MCF-7 cells that were regular polygon- or spindle-shaped. So nucleus and vesicles of MCF-7/ADR cells could be dimly observed. These information mean that the drug resistant cells have changed greatly in order to survive in the presence of ADR.

3.2. QCM dynamic monitoring of the effect of G-Rh_2 and ADR on MCF-7/ADR cells' growth

Fig. 2 shows typical responses of Δf_0 and ΔR_1 to 5×10^4 MCF-7/ADR cells' adhesion, spreading and proliferation on Au electrode and the effect of 1 μmol L^{-1} ADR on cell growth. For comparison, a control experiment was performed by adding 1 mL growth medium without cells. It can be observed that both Δf_0 and ΔR_1 did not change significantly in the following 48 h in the absence of cells. Before the cell addition, the QCM was initially equilibrated with the blank growth medium for 1 h, until stable baselines for Δf_0 and ΔR_1 were achieved. It can be observed that conspicuous decrease in frequency and increase in resistance were presented in 3 h following the cell introduction, corresponding to the adhesion phase of cells. Subsequently the inflexions appeared in QCM-signal curves and continuous frequency decrease and resistance increase were further found, revealing the gradual advent of the latent

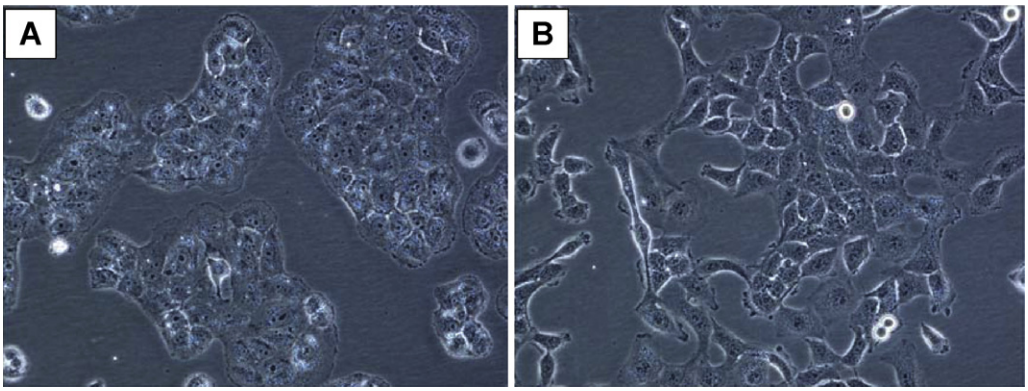

Fig. 1. Microscope images (200×) of MCF-7/ADR cells (A) and MCF-7 cells (B).

phase and the logarithmic growth phase. The most usual quantification principles for the QCM technique include its mass-effect [31], viscodensity-effect [32,33] and stress-effect [34] equations. Living cells are bounded by a "soft" cell membrane and contain with much electrolyte solution inside, which means that they are not rigid. It is reasonably assumed that the attached cells on the QCM surface act as loading of "viscous-membrane-encapsulated" electrolyte solution. In fact, Matsuda et al. indicated that only a very minor fraction of a cell's mass is reflected in the measured frequency shift [35]. These researches have revealed that the mass effect is not appropriate for the analysis of QCM data derived from cell action. The Δf_0 and ΔR_1 values after 48 h induced by MCF-7/ADR cells were about −1080 Hz and 126 Ω, respectively. So the $-\Delta f_0/\Delta R_1$ ratios were calculated to be 8.6 Hz Ω^{-1} on average at the whole cell-culture phase, smaller than the theoretical value for a net viscodensity effect of an AT-cut 9 MHz crystal, 10 Hz Ω^{-1} [36], which means that the QCM responses should be caused by the co-operation of the viscodensity effect and the surface-stress effect [37]. It can be also observed from curve c that cells suffered a normal proliferation process in the presence of 1 μmol mL^{-1} ADR. We even found that 20, 40 and 80 μmol mL^{-1} ADR had no obvious influence on the cell activity (results are not presented here). The above experiments prove distinct multidrug resistance of MCF-7/ADR cells.

Fig. 3 shows the QCM responses to the introduction of 5×10^4 MCF-7/ADR cells and then G-Rh$_2$ at varying concentrations to the culture medium. According to the Δf_0 and ΔR_1 responses, the cell incubation may be roughly divided into two stages, i.e., stage I (1–24 h) and stage II (24–48 h). The addition of G-Rh$_2$ with different concentrations at 24 h caused the obvious transient perturbation signals that were well recovered after ca. 60 min. It seemed that the cellular growth was not influenced by the midway-added 40.0 μmol mL^{-1} G-Rh$_2$. We interestingly found that the changing

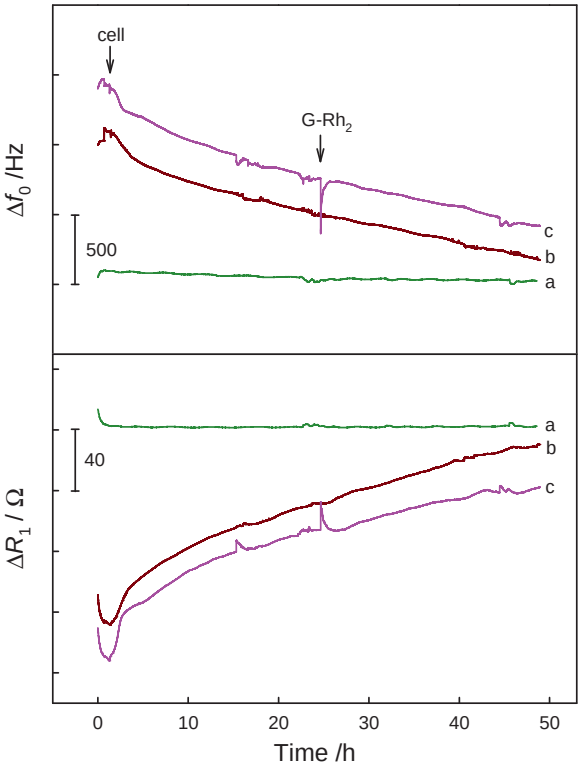

Fig. 2. Real-time Δf_0 and ΔR_1 responses of QCM to the addition of growth medium (a), 5×10^4 MCF-7/ADR cells in the absence (b) and presence (c) of midway-added 1 μmol mL^{-1} ADR.

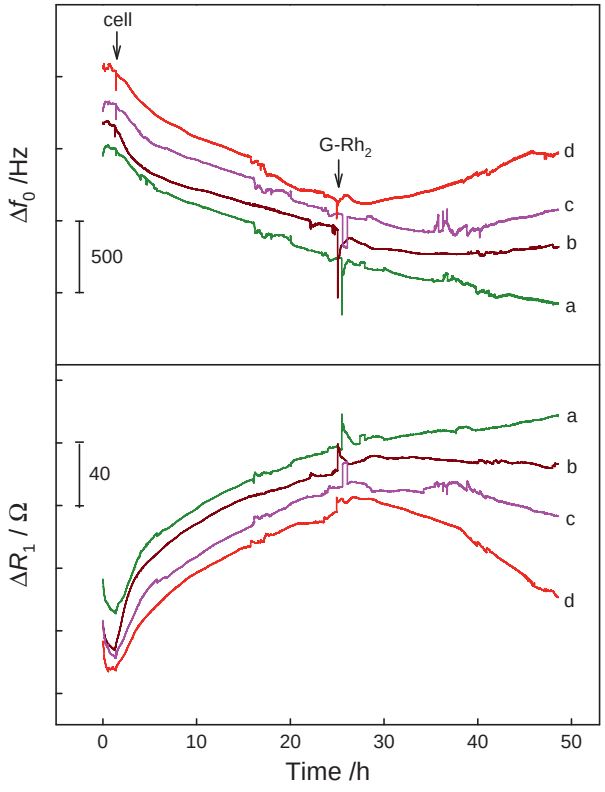

Fig. 3. Real-time Δf_0 and ΔR_1 responses of QCM to the addition of 5×10^4 MCF-7/ADR cells in the presence of midway-added 40 μmol mL^{-1} (a), 80 μmol mL^{-1} (b), 120 μmol mL^{-1} (c) and 160 μmol mL^{-1} (d) G-Rh$_2$.

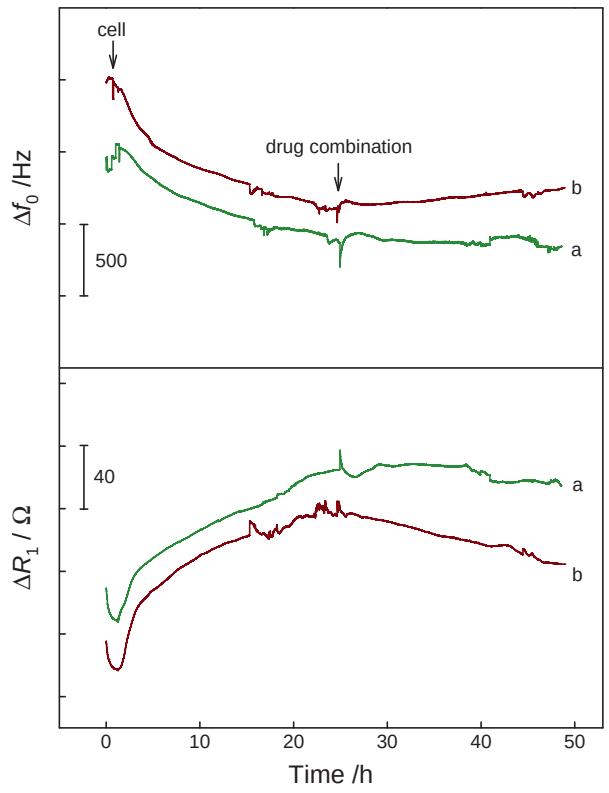

Fig. 4. Real-time Δf_0 and ΔR_1 responses to the addition of 5×10^4 MCF-7/ADR cells in the presence of midway-added 1 μmol mL^{-1} ADR + 40 μmol mL^{-1} G-Rh$_2$ (a) and 1 μmol mL^{-1} ADR + 80 μmol mL^{-1} G-Rh$_2$ (b).

trends of QCM signals were gradually inverted in stage II when the concentration of G-Rh$_2$ was more than 80 μmol L^{-1}. It is reported that the QCM resonant frequency responded proportionally to the surface coverage of cells [26,38]. The cellular coverage should be closely related to cellular growth and proliferation. The more prosperous the cellular growth is, the larger the cellular coverage is, and the larger the Δf_0 and ΔR_1 values are. Once drug inhibits the cellular growth, cell death and the detachment of cells from the substrate occur. Accordingly, the cellular coverage reduces and the QCM signals shrink. Our investigations imply that G-Rh$_2$ with high concentration prevented the proliferation of MCF-7/ADR cells and induced the cellular coverage decreased. The gradually increasing reversal of the Δf_0 and ΔR_1 values from curve a to curve d means that cell-death velocity rose with the increase of drug concentration. After 80 μmol mL^{-1} G-Rh$_2$ was added, the cell death did not appear until 13 h passed. The sustaining time of cell growth was 10 h after introduction of 120 μmol mL^{-1} G-Rh$_2$. The similar period only underwent 3 h in the presence of 160 μmol mL^{-1} G-Rh$_2$. These phenomena indicate that G-Rh$_2$ with higher concentration could act as an effective drug against MCF-7/ADR cells.

The dynamic monitoring of the combinational effect of ADR and G-Rh$_2$ on MCF-7/ADR cells' growth was performed and the results are shown in Fig. 4. It is interesting to be found that the change of QCM signals was at a standstill in the presence of 1 μmol mL^{-1} ADR and 40.0 μmol mL^{-1} G-Rh$_2$ though the two drugs could not lead to cells' death by themselves. The drug combination composed of 1 μmol mL^{-1} ADR and 80 μmol mL^{-1} G-Rh$_2$ resulted in more death of MCF-7/ADR cells, which can be proved by the complete reversal of changing trend in curve b. Furthermore, one can observe that the maintaining time of cell growth before drug-acting in the presence of drug combination was obviously shorter than that in the presence of individual drug. MCF-7/ADR cells almost suffered immediate death once 1 μmol mL^{-1} ADR and 80 μmol mL^{-1} G-Rh$_2$ were added in the growth medium. It is deduced from the above experimental results that the antitumor mechanism of the ADR – G-Rh$_2$ combination was dissimilar to that of individual G-Rh$_2$ and reversal of multidrug resistance in MCF-7/ADR cells could be achieved by G-Rh$_2$.

3.3. Evaluation of the cytotoxicity of ADR and G-Rh$_2$ against MCF-7/ADR cells

As is well known, a drug half-life is the amount of time that it takes for half of the drug to be eliminated from the body and a traditional chemical drug or low molecular weight drug has a half-life of a few to several h. A patient may need to take a new pill or injection several times a day. Therefore, it is significant to study the cytotoxicity of G-Rh$_2$ and drug combination within a short time. Based on the dynamic QCM signals, the inhibition efficiency of drugs, *IE*, can be defined as,

$$IE(\%) = \frac{\Delta f_{0,1} - \Delta f_{0,2}}{\Delta f_{0,1}} \times 100 \quad (1)$$

where $\Delta f_{0,1}$ is the frequency shifts induced by cell-growth in the absence of drug and $\Delta f_{0,2}$ is the frequency changes derived from cell-growth in the presence of G-Rh$_2$ or ADR–G-Rh$_2$ combination, respectively. The inhibition efficiency of G-Rh$_2$ and drug combination on MCF-7/ADR cells' growth at different time after drug introduction were calculated and the results are shown in Table 1. It can be found that the inhibition efficiency increased with the augment of drug contents. The *IE* values at 24 h were higher than those in 12 h, suggesting that the drugs gradually exerted their functions as time went. It is quite obvious that the inhibition efficiency of the drug combination composed of 1 μmol mL^{-1} ADR and 40 μmol mL^{-1} G-Rh$_2$ was very close to that of 120.0 μmol mL^{-1} G-Rh$_2$ at 24 h after drug introduction. The drug combination comprising 1 μmol mL^{-1} ADR and 80 μmol mL^{-1} G-Rh$_2$ exhibited the higher *IE* value at the same time. Interestingly, the drug combinations seemed to have distinct advantages over individual G-Rh$_2$ in cytotoxicity at 12 h. The investigation displayed that the combination of G-Rh$_2$ with ADR at non-effect dosage presented higher cytotoxicity against MCF-7/ADR cells than G-Rh$_2$ alone.

The modified Bürgi formula (i.e., Jin equation) [39], whose concept is universally accepted in pharmacology, was employed to evaluate the cytotoxic effect of the ADR–G-Rh$_2$ combination on MCF-7/ADR cells in the present work.

$$q = \frac{IE_{\text{ADR+G-Rh}_2}}{IE_{\text{ADR}} + IE_{\text{G-Rh}_2} - IE_{\text{ADR}} \times IE_{\text{G-Rh}_2}} \quad (2)$$

where IE$_{\text{ADR}}$, $IE_{\text{G-Rh}_2}$ and $IE_{\text{ADR+G-Rh}_2}$ are the inhibition efficiency of ADR, G-Rh$_2$ and their combination, respectively. The *q* values presenting <0.85, 0.85 ~ 1.25, l.25 ~ 2.0 and >2.0 represent antagonism, simple addition, synergism and apparent synergism, respectively. The *q* values for two drug combinations at different time were calculated and the relevant results are shown in Table 1. The combination of 1 μmol mL^{-1} ADR with 40 μmol mL^{-1} G-Rh$_2$ had the infinite *q* values at 12 h and 24 h after drug introduction, suggesting that this drug combination presented apparent synergism. The other drug combination containing 1 μmol mL^{-1} ADR and 80 μmol mL^{-1} G-Rh$_2$ exhibited the same grade although the *q* values showed tendency to descend. On our opinions, G-Rh$_2$ may find its potential application in tumor therapy based on the synergistic cytotoxicity.

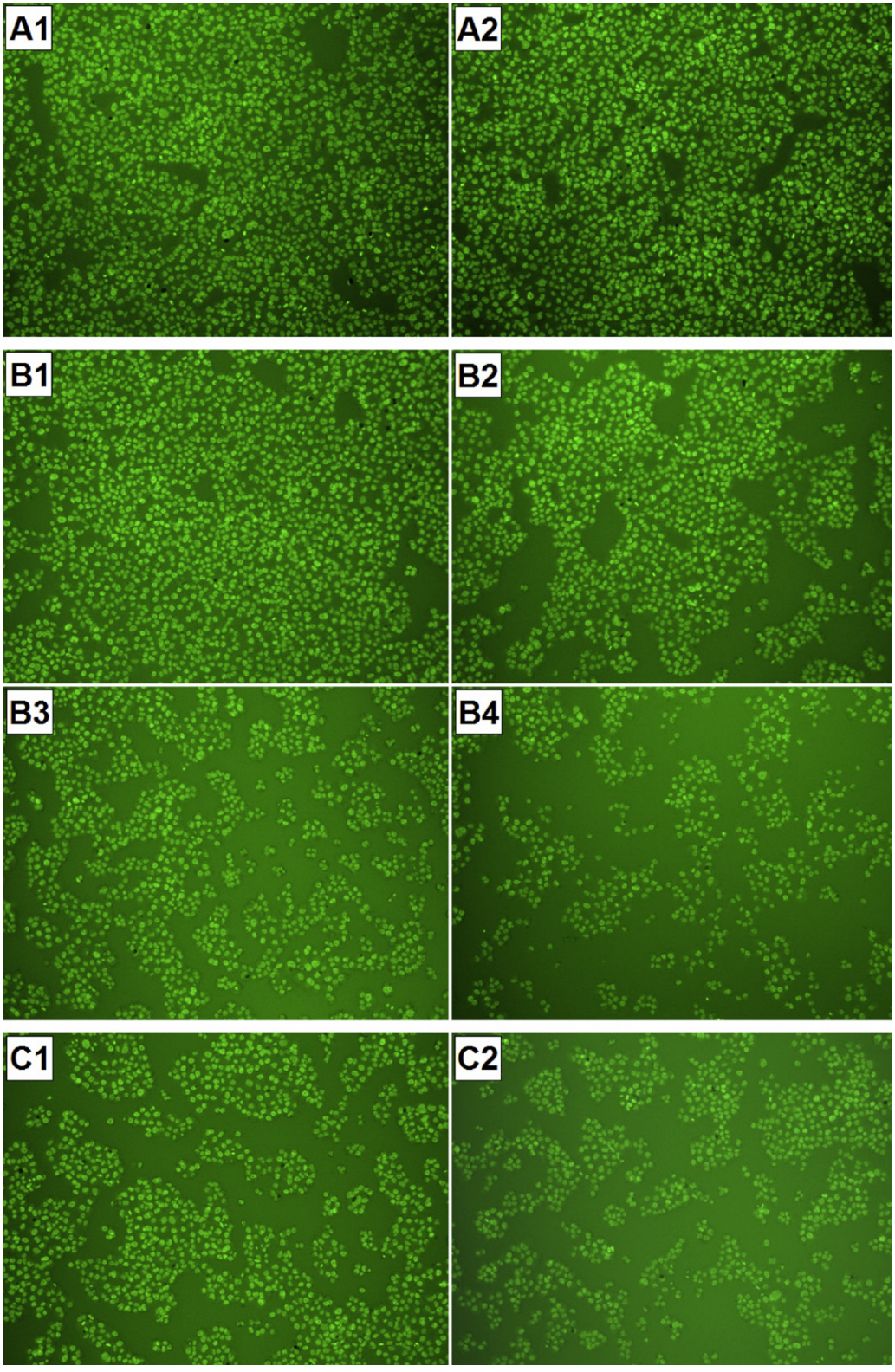

Fig. 5. Fluorescence microscopic images of MCF-7/ADR cells separately incubated with only growth medium as the control (A1), 1 μmol mL^{-1} ADR (A2), 40 μmol mL^{-1} G-Rh$_2$ (B1), 80 μmol mL^{-1} G-Rh$_2$ (B2), 120 μmol mL^{-1} G-Rh$_2$ (B3), 160 μmol mL^{-1} G-Rh$_2$ (B4), 1 μmol mL^{-1} ADR + 40 μmol mL^{-1} G-Rh$_2$ (C1), and 1 μmol mL^{-1} ADR + 80 μmol mL^{-1} G-Rh$_2$ (C2) for 24 h. The magnification is 100×. The concentration of initially added cell: 5.0×10^4 cells.

3.4. Cell viability study by fluorescent microscopic inspection and MTT assay

The cell viability in the presence of drug and drug combination were also investigated by fluorescent microscopic measurement and MTT assay, respectively. Fig. 5A1, A2, B1–B4 and C1–C2 shows microscopic fluorescent images of MCF-7/ADR separately incubated with growth medium, ADR, G-Rh$_2$ and drug combination for 24 h, respectively. The cell-action information revealed by the series of modality-photos are well comparable with those revealed

Table 1
The *IE* and *q* values at different time after drug introduction.

Drug content in growth medium	*IE* (%) at 12 h after drug introduction	RSD (%)	*q*	*IE* (%) at 24 h after drug introduction	RSD (%)	*q*
80 μmol mL^{-1} G-Rh$_2$	5.32	3.3	–	22.2	3.8	–
120 μmol mL^{-1} G-Rh$_2$	8.51	2.2	–	32.4	4.3	–
160 μmol mL^{-1} G-Rh$_2$	20.0	4.1	–	62.6	5.7	–
1 μmol mL^{-1} ADR + 40 μmol mL^{-1} G-Rh$_2$	21.4	5.6	∞	31.0	4.7	∞
1 μmol mL^{-1} ADR + 80 μmol mL^{-1} G-Rh$_2$	30.1	3.8	5.66	46.0	5.0	2.07

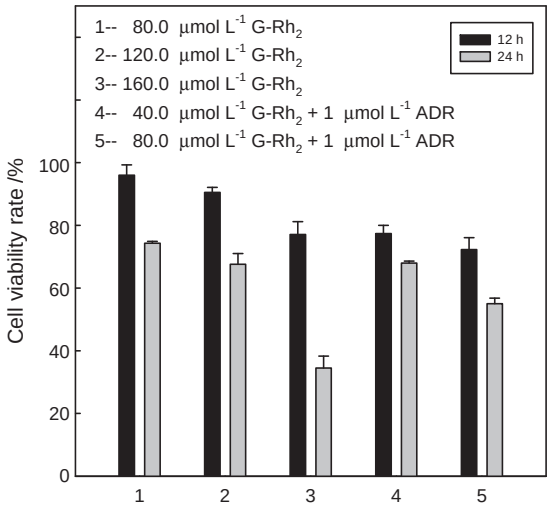

Fig. 6. The cell viability of MCF-7/ADR cells cultured in different wells tested by MTT assay at 12 and 24 h after drug introduction (data presented are mean S.D., $n = 3$).

by the QCM measurement. MCF-7/ADR cells were basically distributed on the substrate as a monolayer in the absence of drug. Panels A2 and B1 reveal that the cell could remain normal growth in the presence of 1 μmol mL^{-1} ADR or 40.0 μmol mL^{-1} G-Rh$_2$. The amounts of cells suffering proliferation decreased with the increase of G-Rh$_2$ concentration in growth medium. Few cells occupied less than half substrate area when the G-Rh$_2$ concentration was relatively higher. The cell number in panel C1 were found to be approximately equal to that in panel B3 and the less cells were presented in panel C2, which further proved that the synergistic cytotoxicity of drug combination.

The cell viability was quantitatively evaluated by MTT assay. MTT is metabolized to a purple formazan salt by mitochondrial enzymes in living cells, and the absorbance is thus proportional to the number of viable cells. In this work, the cell viability was defined as the ratio of the absorbance at 570 nm obtained from the well in which cells were incubated with G-Rh$_2$ or ADR–G-Rh$_2$ combination to that derived from the well in which cells grew in the absence of drug. As we know, the bigger the inhibition efficiency is, the smaller the cell viability is. It can be observed that the information revealed by Fig. 6 were basically in compliance with those presented in Table 1.

4. Conclusion

In this work, the real-time monitoring of the drug-induced death process of MCF-7/ADR cells was performed with QCM measurement. It is found that G-Rh$_2$ could effectively inhibit the proliferation of MCF-7/ADR cells when the drug concentration was more than 80 μmol L^{-1}. The combination of G-Rh$_2$ with ADR at non-effect dosage resulted in the higher inhibition efficiencies and the increased cell-death velocity than individual G-Rh$_2$ and presented apparent synergism in the evaluation of drug combination. The QCM method was validated by comparison with classical fluorescent microscopic inspection and MTT assay. The research indicates that reversal of multidrug resistance in MCF-7/ADR cells could be achieved by G-Rh$_2$ and active components in natural medicinal plants may find more application in multidrug resistance research in future.

Acknowledgments

This work was supported by the National Science Foundation of China (20905025, 21145001, 20975037, and 20705008), the State Special Scientific Project on Water Treatment (2009ZX07212-001-06), the Scientific Research Fund of Hunan Provincial Education Department (09B062) and Aid program for Science and Technology Innovative Research Team in Higher Educational Institutions of Hunan Province.

References

[1] A. Persidis, Nat. Biotechnol. 17 (1999) 94–95.
[2] C. Muller, J.D. Bailly, F. Goubin, J. Laredo, J.P. Jaffrezou, C. Bordier, G. Laurent, Int. J. Cancer 56 (1994) 749–754.
[3] S. Toma, G. Maselli, G. Dastoli, E.D. Francisci, P. Raffo, Cancer Lett. 116 (1997) 103–110.
[4] T. Naruse, Y. Nishida, N. Ishiguro, Biomed. Pharmacother. 61 (2007) 338–346.
[5] X. Wan, G. Sun, H. Wang, S. Xu, Z. Wang, S. Liu, Dig. Liver Dis. 40 (2008) 531–539.
[6] S. Shibata, J. Korean Med. Sci. 16 (2001) S28–S37.
[7] E.K. Park, M.K. Choo, E.J. Kim, M.J. Han, D.H. Kim, Biol. Pharm. Bull. 26 (2003) 1581–1584.
[8] H.Y. Kwon, E.H. Kim, S.W. Kim, S.N. Kim, J.D. Park, D.K. Rhee, Arch. Pharm. Res. 31 (2008) 171–177.
[9] I. Kitagawa, M. Yoshikawa, M. Yoshihara, T. Hayashi, T. Taniyama, Yakugaku Zasshi 103 (1983) 612–622.
[10] H. Nakata, Y. Kikuchi, T. Tode, J. Hirata, T. Kita, K. Ishii, K. Kudoh, I. Nagata, N. Shinomiya, Jpn. J. Cancer Res. 89 (1998) 733–740.
[11] S. Odashima, T. Ohta, H. Kohno, Cancer Res. 45 (1985) 2781–2784.
[12] K. Fujikawa-Yamarnoto, T. Ota, S. Odashima, H. Abe, S. Arichi, Cancer J. 1 (1987) 349–352.
[13] B. Li, J. Zhao, C. Wang, J. Searle, T. He, C. Yuan, W. Du, Cancer Lett. 301 (2011) 185–192.
[14] S. Choi, T.W. Kim, S.V. Singh, Pharm. Res. 26 (2009) 2280–2288.
[15] J.I. Oh, K.H. Chun, S.H. Joo, Y.T. Oh, S.K. Lee, Cancer Lett. 230 (2005) 228–238.
[16] H.E. Kim, J.H. Oh, S.K. Lee, Y.J. Oh, Life Sci. 65 (1999) 33–40.
[17] Y.S. Kim, S.H. Jin, Arch. Pharm. Res. 27 (2004) 834–839.
[18] X.F. Fei, B.X. Wang, S. Tashiro, T.J. Li, J.S. Ma, T. Ikejima, Acta Pharmacol. Sin. 23 (2002) 315–322.
[19] W.W.G. Jia, X.X. Bu, D. Philips, H. Yan, G.Y. Liu, X.G. Chen, J. Bush, G. Li, Can. J. Physiol. Pharmacol. 82 (2004) 431–437.
[20] X.W. Xie, A. Eberding, C. Madera, L. Fazli, W. Jia, L. Goldenberg, M. Gleave, E.S. Guns, J. Urol. 175 (2006) 1926–1931.
[21] H.T. Xie, G.J. Wang, M. Chen, X.L. Jiang, H. Li, H. Lv, C.R. Huang, R. Wang, M. Roberts, Biol. Pharm. Bull. 28 (2005) 383–386.
[22] J. Jin, S. Shahi, H.K. Kang, H.W. van Veen, T.P. Fan, Biochem. Biophys. Res. Commun. 345 (2006) 1308–1314.
[23] A. Janshoff, H.J. Galla, C. Steinem, Angew. Chem. Int. Ed. 39 (2000) 4004–4032.
[24] K.A. Marx, Biomacromolecules 4 (2003) 1099–1120.
[25] Z. Lin, M.D. Ward, Anal. Chem. 67 (1995) 685–693.
[26] J. Redepenning, T.K. Schlesinger, E.J. Mechalke, D.A. Puleo, R. Bizios, Anal. Chem. 65 (1993) 3378–3381.
[27] L. Tan, X. Jia, X. Jiang, Y. Zhang, H. Tang, S. Yao, Q. Xie, Anal. Biochem. 383 (2008) 130–136.
[28] M.S. Lord, C. Modin, M. Foss, M. Duch, A. Simmons, F.S. Pedersen, F. Besenbacher, B.K. Milthorp, Biomaterials 29 (2008) 2581–2587.
[29] J. Fatisson, F. Azari, N. Tufenkji, Biosens. Bioelectron. 26 (2011) 3207–3212.
[30] L. Tan, X. Jia, X. Jiang, Y. Zhang, H. Tang, S. Yao, Q. Xie, Biosens. Bioelectron. 24 (2009) 2268–2272.

[31] G. Sauerbrey, Z. Phys. 155 (1959) 206–222.
[32] K.K. Kanazawa, J.G. Gordon, Anal. Chem. 57 (1985) 1770–1771.
[33] V.E. Granstaff, S.J. Martin, J. Appl. Phys. 75 (1994) 1319–1329.
[34] E.P. EerNisse, J. Appl. Phys. 43 (1972) 1330–1337.
[35] T. Matsuda, A. Kishida, H. Ebato, Y. Okahata, ASIO J. (1992) M1771.
[36] E.J. Calvo, C. Danilowicz, R.J. Etchenique, Chem. Soc. Faraday Trans. 91 (1995) 4083–4091.
[37] L. Tan, Q. Xie, X. Jia, M. Guo, Y. Zhang, H. Tang, S. Yao, Biosens. Bioelectron. 24 (2009) 1603–1609.
[38] X. Jia, Z. Zhang, L. Tan, Y. Zhang, Q. Xie, S. Yao, Chin. Chem. Lett. 17 (2006) 509–512.
[39] Z. Jin, Acta Pharmacol. Sin. 25 (2004) 146–147.